Simultaneous Measurement of $^3J_{HN,H\alpha}$ and $^3J_{H\alpha,H\beta}$ Coupling Constants in $^{13}C,^{15}N$-Labeled Proteins

Frank Löhr,[†] Jürgen M. Schmidt,[‡] and Heinz Rüterjans*[,†]

Contribution from the Institut für Biophysikalische Chemie, Johann Wolfgang Goethe-Universität, Biozentrum N230, Marie Curie-Strasse 9, 60439 Frankfurt am Main, Germany, and Division of Molecular Structure, National Institute for Medical Research, Mill Hill, London NW7 1AA, United Kingdom

Received April 26, 1999. Revised Manuscript Received October 20, 1999

Abstract: A triple-resonance NMR pulse sequence termed HA[HB,HN](CACO)NH is proposed that provides two types of $^3J_{HH}$ coupling constants sharing the C^α proton in amino acid spin systems. The experiment is of the quantitative *J* correlation-type and takes advantage of the favorable relaxation properties of $^1H^a-^{13}C^\alpha$ multiple-quantum coherence as compared to schemes relying on antiphase magnetization. The problem of signal overlap is considerably reduced by calculating *J* values from cross-peak−cross-peak intensity ratios rather than referencing diagonal peaks. Application to flavodoxin from *Desulfovibrio vulgaris* yields a total of 282 $^3J_{H\alpha,H\beta}$ and $^3J_{HN,H\alpha}$ coupling constants, normally determined in two separate experiments, to be used in conjunction with heteronuclear couplings to derive angular constraints for the protein's backbone and side chains. While $^3J_{H\alpha,H\beta}$ coupling constants indicate some extent of conformational averaging not in accord with fixed side chain torsion, excellent correlation of the experimental $^3J_{HN,H\alpha}$ values with X-ray derived ϕ torsional angles in flavodoxin is observed.

Introduction

In the analysis of biomolecular structure by NMR spectroscopy, $^3J_{HN,H\alpha}$ and $^3J_{H\alpha,H\beta}$ are among those vicinal proton−proton couplings in amino acid spin systems to deliver most valuable information on torsion angles ϕ and χ^1, respectively.[1,2] Pairs of $^3J_{H\alpha,H\beta}$ coupling constants are also critical to the stereospecific resonance assignment of C^β-bound methylene protons. Direct extraction of ^1H, ^1H coupling constants from signal splittings is impeded in 1D sections of spectra of biological macromolecules as proton line widths usually exceed the size of the *J* couplings. Alternatively, they are obtained from two-dimensional E.COSY[3] or P.E.COSY[4] spectra, the application of which is usually restricted to comparatively low molecular weight compounds because of limited sensitivity and spectral dispersion. Multidimensional heteronuclear E.COSY-type experiments[5] relying on ^{15}N and/or ^{13}C isotope-labeled recombinant proteins proved particularly useful for the determination of both $^3J_{HN,H\alpha}$[6,7] and $^3J_{H\alpha,H\beta}$[7,8] couplings as ^3J doublet components become separated by exploiting large one-bond splittings in orthogonal spectral dimensions, e.g. in HNCA-E.COSY (for $^3J_{HN,H\alpha}$) or HCCH-E.COSY (for $^3J_{H\alpha,H\beta}$).

Based on the fact that protein backbone amide protons usually possess a single homonuclear coupling partner, $^3J_{HN,H\alpha}$ coupling constants are, however, more conveniently and often more accurately measured in proton−nitrogen correlation spectra by fitting $^1H-^{15}N$ correlation as subject to *J* modulation in either the frequency[9] or the time[10,11] domain, whereby line width effects are taken into account. In a spin−echo difference approach, *J* values have been derived from intensity ratios of $^1H-^{15}N$ cross-peaks in 2D spectra recorded with and without decoupling of α-protons.[12]

Eventually, homonuclear coupling constants are measured in quantitative *J* correlation experiments employing "in-phase

* Address correspondence to this author at the Institut für Biophysikalische Chemie, Johann Wolfgang Goethe-Universität.

† Institut für Biophysikalische Chemie, University Frankfurt.

‡ Division of Molecular Structure, NIMR London.

(1) Karplus, M. *J. Am. Chem. Soc.* **1963**, *85*, 2870−2871.

(2) Bystrov, V. F. *Prog. NMR Spectrosc.* **1976**, *10*, 41−81.

(3) Griesinger, C.; Sørensen, O. W.; Ernst, R. R. *J. Am. Chem. Soc.* **1985**, *107*, 6394−6396.

(4) Mueller, L. *J. Magn. Reson.* **1987**, *72*, 191−196.

(5) (a) Montelione, G. T.; Winkler, M. E.; Rauenbühler, P.; Wagner, G. *J. Magn. Reson.* **1989**, *82*, 198−204. (b) Wider, G.; Neri, D.; Otting, G.; Wüthrich, K. *J. Magn. Reson.* **1989**, *85*, 426−431. (c) Montelione, G. T.; Emerson, S. D.; Lyons, B. A. *Biopolymers* **1992**, *32*, 327−334.

(6) (a) Montelione, G. T.; Wagner, G. *J. Am. Chem. Soc.* **1989**, *111*, 5474−5475. (b) Schmieder, P.; Thanabal, V.; McIntosh, L. P.; Dahlquist, F. W.; Wagner, G. *J. Am. Chem. Soc.* **1991**, *113*, 6323−6324. (c) Seip, S.; Balbach, J.; Kessler, H. *Angew. Chem., Int. Ed. Engl.* **1992**, *31*, 1609−1611. (d) Görlach, M.; Wittekind, M.; Farmer, B. T., II; Kay, L. E.; Mueller, L. *J. Magn. Reson., B* **1993**, *101*, 194−197. (e) Madsen, J. C.; Sørensen, O. W.; Sørensen, P.; Poulsen, F. M. *J. Biomol. NMR* **1993**, *3*, 239−244. (f) Weisemann, R.; Rüterjans, H.; Schwalbe, H.; Schleucher, J.; Bermel, W.; Griesinger, C. *J. Biomol. NMR* **1994**, *4*, 231−240. (g) Löhr, F.; Rüterjans, H. *J. Biomol. NMR* **1995**, *5*, 25−36. (h) Meissner, A.; Duus, J. Ø.; Sørensen, O. W. *J. Magn. Reson.* **1997**, *128*, 92−97. (i) Sørensen, M. D.; Meissner, A.; Sørensen, O. W. *J. Biomol. NMR* **1997**, *10*, 181−186. (j) Meissner, A.; Schulte-Herbrüggen, T.; Sørensen, O. W. *J. Am. Chem. Soc.* **1998**, *120*, 3803−3804.

(7) Sørensen, O. W. *J. Magn. Reson.* **1990**, *90*, 433−438.

(8) (a) Gemmecker, G.; Fesik, S. W. *J. Magn. Reson.* **1991**, *95*, 208−213. (b) Griesinger, C.; Eggenberger, U. *J. Magn. Reson.* **1992**, *97*, 426−434. (c) Emerson, S. D.; Montelione, G. T. *J. Am. Chem. Soc.* **1992**, *114*, 354−356. (d) Emerson, S. D.; Montelione, G. T. *J. Magn. Reson.* **1992**, *99*, 413−420. (e) Eggenberger, U.; Karimi-Nejad, Y.; Thüring, H.; Rüterjans, H.; Griesinger, C. *J. Biomol. NMR* **1992**, *2*, 583−590. (f) Olsen, H. B.; Ludvigsen, S.; Sørensen, O. W. *J. Magn. Reson., A* **1993**, *105*, 321−322.

(9) (a) Kay, L. E.; Bax, A. *J. Magn. Reson.* **1990**, *86*, 110−126. (b) Forman-Kay, J. D.; Gronenborn, A. M.; Kay, L. E.; Wingfield, P. T.; Clore, G. M. *Biochemistry* **1990**, *29*, 1566−1572.

(10) (a) Neri, D.; Otting, G.; Wüthrich, K. *J. Am. Chem. Soc.* **1990**, *112*, 3663−3665. (b) Billeter, M.; Neri, D.; Otting, G.; Qian, Y. Q.; Wüthrich, K. *J. Biomol. NMR* **1992**, *2*, 257−274. (c) Szyperski, T.; Güntert, P.; Otting, G.; Wüthrich, K. *J. Magn. Reson.* **1992**, *99*, 552−560.

(11) Kuboniwa, H.; Grzesiek, S.; Delaglio, F.; Bax, A. *J. Biomol. NMR* **1994**, *4*, 871−878.

(12) Ponstingl, H.; Otting, G. *J. Biomol. NMR* **1998**, *12*, 319−324.

10.1021/ja991356h CCC: $18.00
Published on Web 12/04/1999

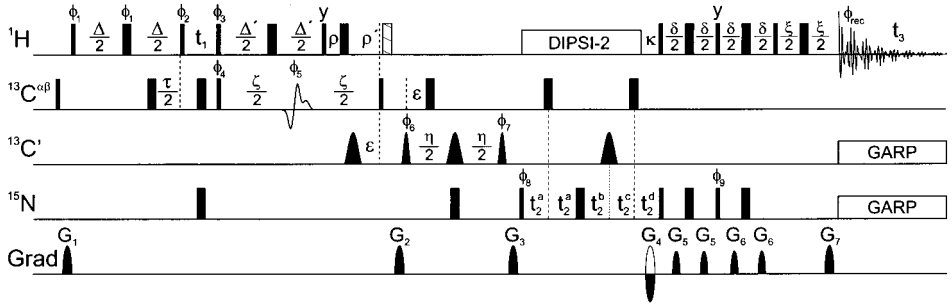

Figure 1. Pulse scheme for the HA[HB,HN](CACO)NH experiment. Narrow and wide pulses have flip angles of 90° and 180°, respectively, and are applied with phase *x* unless specified. Proton pulses are applied at the water resonance (4.75 ppm) with an RF field strength of 30 kHz except DIPSI-2[16] decoupling ($\gamma B_2 = 4.5$ kHz) which is applied at the center of the amide region (8.5 ppm). The hatched bar denotes a spin-lock pulse with a duration of 500 μs. The carrier frequencies for pulses on carbonyl and α-carbons correspond to 176 and 58 ppm, respectively. The initial three carbon pulses are applied with an RF field strength of 18 kHz whereas the widths of the remaining rectangular pulses are adjusted to minimize excitation of the carbonyl region ($\tau_{90}° = 54.3$ μs, $\tau_{180}° = 48.6$ μs at 151 MHz ^{13}C). All carbonyl-selective pulses are shaped according to the center lobe of a sin(*x*)/*x* function with a duration of 124 μs. To avoid nonresonant effects on α-carbons, the first 180° ^{13}C′ pulse is in addition cosine-modulated such that it has two excitation maxima at ±118 ppm from the center of the ^{13}Cα region.[17] Empirical adjustment of the phase ϕ_7 compensates for zero-order phase shifts of ^{13}C′ magnetization induced by the 180° ^{13}Cα pulse in the η period. The shaped 180° pulse in the center of the ζ delay is a 250 μs G3 Gaussian cascade[18] applied at 48 ppm using phase modulation.[19] Decoupling during acquisition is achieved by GARP-1[20] modulation using RF field strengths of 1 (^{13}C′) and 0.75 kHz (^{15}N). ^{15}N chemical shifts evolve in a semiconstant-time manner,[21] i.e., the presence of transverse ^{15}N magnetization increases as a function of t_2 from its initial value $T_N = 30.25$ ms to the final length of the acquisition time (AT) according to $t_2^a = (T_N - \chi t_2)/4$; $t_2^b = [(1 - \chi)t_2]/2$; $t_2^c = (T_N + \chi t_2)/4$; $t_2^d = [T_N + (2 - \chi)t_2]/4$, where $\chi = T_N/\mathrm{AT}$. Delays are $\Delta = 15$ ms; $\Delta' = 19$ ms; $\tau = 3.5$ ms; $\zeta = 26.4$ ms; $\rho = (\zeta - \Delta' - \tau)/2 = 1.95$ ms; $\rho' = (\zeta - \Delta' + \tau)/2 = 5.45$ ms; $\epsilon = 4.6$ ms; $\eta = 22$ ms; $\kappa = 5.4$ ms; $\delta = 5$ ms; and $\xi = 1.4$ ms. Phase cycling is $\phi_1 = x,-x$; $\phi_2 = 4(x), 4(-x)$; $\phi_3 = 8(x), 8(-x)$; $\phi_4 = 2(x), 2(-x)$; $\phi_5 = 2(x,-x), 2(y,-y)$; $\phi_6 = 8(x),8(-x)$; $\phi_7 = x + 51°$; $\phi_8 = x$; $\phi_9 = y$; $\phi_{receiver} = R, 2(-R), R$ with $R = x, 2(-x), x$. Quadrature detection in t_1 is accomplished by altering ϕ_1 and ϕ_2 in the States-TPPI[22] manner. All gradients are sine-bell shaped and have durations of 1 ms ($G_{1,2,3,4}$) or 0.5 ms ($G_{5,6,7}$) with directions and approximate strengths at their center G_1: *x*, 10 G/cm; G_2: *z*, 12.5 G/cm; G_3: *y*, 7.5 G/cm; G_4: *z*, −39.4 G/cm; G_5: *x*, 4 G/cm, *y*, 5.5 G/cm; G_6: *x*, 5.5 G/cm, *y*, 4 G/cm; G_7: *z*, 8 G/cm. N- and P-type signals are collected alternately by inverting the direction of G_4 along with ϕ_9. Axial peaks are shifted to the edge of the spectrum by incrementing ϕ_8 and the receiver phase by 180° for each value of t_2.

COSY" magnetization transfer to encode coupling magnitudes in intensity ratios of cross and diagonal peaks.[13] Examples include HNHA[11,14] and HACAHB-COSY[15] pulse sequences both of which emerged as standard methods in protein structure determination and provide reliable values for $^3J_{HN,H\alpha}$ and $^3J_{H\alpha,H\beta}$, respectively.

As protein sizes become larger, the major drawback of both these latter methods is the chance of overlap of reference diagonal signals needed for proper *J*-coupling calculation. A particular disadvantage of the HACAHB-COSY experiment is the critical detection of H^α magnetization requiring samples be dissolved in D_2O while lacking appropriate schemes to suppress the otherwise intense residual solvent signal.

Here we propose a strategy first to simultaneously determine both couplings $^3J_{HN,H\alpha}$ and $^3J_{H\alpha,H\beta}$ in a single experiment and second to quantitate *J*-coupling constants from intensity ratios of cross-peak pairs avoiding the mentioned problem of diagonal peak overlap. As H^N magnetization is recorded during data acquisition, the experiment must be carried out in fully protonated solvent.

Experimental Section

All NMR spectra were recorded on a Bruker DMX-600 spectrometer equipped with a $^1H\{^{13}C,^{15}N\}$ triple-resonance probe containing self-shielded *xyz*-gradient coils. The temperature was set at 27 °C. The HA[HB,HN](CACO)NH experiment acquired according to the pulse scheme of Figure 1 used a 1.4 mM sample of recombinant, uniformly ^{13}C/^{15}N labeled *Desulfovibrio vulgaris* flavodoxin dissolved in 10 mM potassium phosphate buffer (pH 7.0) containing 5% D_2O. A total of 112 × 36 × 768 complex data points (t_1, t_2, t_3) were recorded corresponding to acquisition times of 19.1, 40.2, and 86.7 ms, respectively. Spectral widths were 9.8 (F_1, ^{1}H), 14.7 (F_2, ^{15}N), and 14.8 ppm (F_3, ^{1}H). Accumulation of 16 scans per FID resulted in a measuring time of 69 h. Linear prediction was applied to extend the time-domain data by 40% in the ^{15}N dimension. Data in all three dimensions were multiplied with a squared-cosine weighting function and zero-filled prior to Fourier transformation to obtain digital resolutions of 5.7, 7.0, and 4.3 Hz (F_1, F_2, F_3).

Reference $^3J_{HN,H\alpha}$ coupling constants were measured with a HNHA experiment employing the pulse sequence of ref 11 with the final jump-and-return pulse pair replaced by a WATERGATE[23] sequence. The *J*-evolution delay 2ξ was adjusted to 17 ms. Data acquisition in the ^{15}N dimension was limited to 24 complex points (25.7 ms). Spectral parameters in F_1 and F_3 and processing were identical with those used in the HA[HB,HN](CACO)NH. The spectrum was recorded within 64 h using a 4 mM sample of ^{15}N-labeled flavodoxin.

Reference $^3J_{H\alpha,H\beta}$ coupling constants in flavodoxin were obtained from HACAHB-COSY as well as HC(C)H−E.COSY experiments applied to the ^{13}C/^{15}N labeled sample in H_2O. The

(13) Bax, A.; Vuister, G. W.; Grzesiek, S.; Delaglio, F.; Wang, A. C.; Tschudin, R.; Zhu, G. *Methods Enzymol.* **1994**, *239*, 79−105.
(14) Vuister, G. W.; Bax, A. *J. Am. Chem. Soc.* **1993**, *115*, 7772−7777.
(15) Grzesiek, S.; Kuboniwa, H.; Hinck, A. P.; Bax, A. *J. Am. Chem. Soc.* **1995**, *117*, 5312−5315.
(16) Shaka, A. J.; Lee, C. J.; Pines, A. *J. Magn. Reson.* **1988**, *77*, 274−293.
(17) McCoy, M. A.; Mueller, L. *J. Magn. Reson.* **1992**, *99*, 18−36.
(18) Emsley, L.; Bodenhausen, G. *Chem. Phys. Lett.* **1990**, *165*, 469−476.
(19) Patt, S. *J. Magn. Reson.* **1992**, *96*, 94−102.
(20) Shaka, A. J.; Barker, P. B.; Freeman, R. *J. Magn. Reson.* **1985**, *64*, 547−552.
(21) (a) Logan, T. M.; Olejniczak, E. T.; Xu, R. X.; Fesik, S. W. *FEBS Lett.* **1992**, *314*, 413−418. (b) Grzesiek, S.; Bax, A. *J. Biomol. NMR* **1993**, *3*, 185−204.
(22) Marion, D.; Ikura, M.; Tschudin, R.; Bax, A. *J. Magn. Reson.* **1989**, *85*, 393−399.
(23) Piotto, M.; Saudek, V.; Sklenář, V. *J. Biomol. NMR* **1992**, *2*, 661−665.

HACAHB−COSY employed the pulse scheme of ref 15 supplemented with presaturation to suppress the water resonance. The period 2δ for the de- and rephasing of proton−proton couplings was set at 17 ms. Time domain data consisted of 76 ($^{13}C^{\alpha}$) × 66 (^1H) × 256 ($^1H^{\alpha}$) complex points, corresponding to acquisition times of 19.2 (t_1), 12.3 (t_2), and 85.2 ms (t_3). Co-addition of 16 scans for each FID required a spectrometer time of 88 h. The three-dimensional HC(C)H-E.COSY experiment was based on the pulse sequence in ref 8f which includes a DEPT-type $^{13}C-^1H$ coherence transfer. The ^1H β-pulse had a flip angle of 30°. Acquisition times were 13.5 (t_1), 14.1 (t_2), and 87.0 ms (t_3) in the H^{α}, C^{α}, and H^{β} dimensions, respectively. Sixteen scans per FID were recorded giving rise to a net measurement time of 93 h.

The effect of passive spin flips on $^3J_{HN,H\alpha}$ coupling constants measured with the HA[HB,HN](CACO)NH method was assessed by obtaining selective H^N T_1 relaxation times from the exponential decay of H^N auto-correlation peak intensities in a series of 2D $^1H\{^{15}N\}$-HSQC-NOESY spectra as proposed by Peng and Wagner.[24] Within 43 h, a total of 16 spectra were recorded using the ^{15}N-labeled protein sample in an interleaved manner with NOE mixing periods ranging from 10 to 310 ms.

Results and Discussion

The pulse sequence shown in Figure 1 basically consists of an $^1H,^1H$ in-phase COSY element[15] incorporated in the H(CACO)NH[25] triple-resonance sequence. In the novel scheme, unlike previous quantitative *J* correlation experiments, magnetization starts out from the central spin (H^{α}) of a linear proton-coupling network and fans out into two directions. During the initial Δ period H^{α} antiphase magnetization builds up with respect to the directly bonded carbon and both scalar coupled protons H^{β} and H^N. Following the 90° (ϕ_2) pulse, both cross-peak ($^1H^{\beta}$, $^1H^N$) and auto peak ($^1H^{\alpha}$) chemical shifts evolve in t_1. The subsequent pair of $^1H/^{13}C$ 90° pulses creates $^1H^{\alpha}-^{13}C^{\alpha}$ multiple-quantum coherence. To take advantage of its favorable relaxation properties compared to either $^1H^{\alpha}$ or $^{13}C^{\alpha}$ single-quantum coherences[15,26] proton antiphase magnetization with respect to its homonuclear coupling partners refocuses during a period Δ' while carbon antiphase magnetization simultaneously builds up with respect to $^{13}C'$. To account for the faster transverse relaxation of H^{α} single-quantum coherence the dephasing period Δ is shorter than the rephasing period Δ'. Delay Δ' can be prolonged with no effect on the overall duration of the pulse sequence as it readily fits the fixed ζ delay, adjusted to $(^1J_{C\alpha,C\beta})^{-1}$ to remove effects of passive $C^{\alpha}-C^{\beta}$ couplings on the signal amplitude. A short proton purge pulse followed by a pulsed-field gradient destroys residual ^1H magnetization components. Following a relay step via peptidyl carbonyl nuclei, the final reverse INEPT sequence, a combination of the sensitivity enhancement scheme[27] and gradient coherence selection,[28] transfers magnetization from the nitrogen to the amide proton of the subsequent residue, where it is readily detected.

The novel pulse sequence, referred to as HA[HB,HN](CACO)NH, has been applied to oxidized *Desulfovibrio vulgaris* flavodoxin, a bacterial redox protein consisting of 147 amino acid residues and a flavin−mononucleotide cofactor. Figure 2 shows slices from the resulting 3D spectrum each containing one auto peak at the $\omega_1(H^{\alpha})$ position and up to three cross-peaks (at $\omega_1(H^N)$ or $\omega_1(H^{\beta})$) depending on the amino acid type and the size of the homonuclear couplings. Vicinal coupling constants are calculated from the amplitude ratio of cross (I_C) and auto peaks (I_A)

$$I_C/I_A = -\tan(\pi J_{HH}\Delta)\tan(\pi J_{HH}\Delta') \quad (1)$$

approximated by

$$I_C/I_A = -\tan^2[\pi J_{HH}(\Delta + \Delta')/2] \quad (2)$$

with an error of typically less than 1% for couplings between 2 and 12 Hz with $\Delta = 15$ ms and $\Delta' = 19$ ms. Amide cross-peak intensities are affected by the D_2O content of the sample, requiring raw $^3J_{HN,H\alpha}$ values be corrected. Here, all $^1H^N$ (F1) cross-peak intensities were divided by 0.95, for simplicity assuming the D/H exchange to be uniform and at equilibrium. Note that auto peaks and H^{β} cross-peaks can still be detected for amino acids where the amide proton has been exchanged for a deuteron because the magnetization is finally transferred to the amide of the subsequent residue.

For the 129 nonglycine residues of flavodoxin, 119 $^3J_{HN,H\alpha}$ and 163 $^3J_{H\alpha,H\beta}$ coupling constants ranging from 2.0 to 9.9 Hz and 2.5 to 11.3 Hz, respectively, were obtained, and in 19 further instances an upper limit for *J* could be derived from the absence of cross-peaks. In contrast, only 100 $^3J_{HN,H\alpha}$ values were measured in the HNHA spectrum and 83 and 138 $^3J_{H\alpha,H\beta}$ coupling constants resulted from the evaluation of HACAHB-COSY and HC(C)H-E.COSY spectra, respectively. The lower efficiency of the latter experiments can be mainly attributed to increased spectral overlap. For the purpose of comparison, the same flavodoxin sample dissolved in 95% H_2O has been used in the reference HACAHB-COSY, normally requiring a ^{13}C-labeled sample in D_2O to cope with interference from the strong residual water signal.

As shown in Figure 3A, apparent $^3J_{HN,H\alpha}$ coupling constants from both HA[HB,HN](CACO)NH and HNHA spectra agree reasonably, the largest deviation being 1.7 Hz. Linear regression delivered slope and intercept of 1.00 and 0.32 Hz, pointing out that *J* values from HA[HB,HN](CACO)NH are slightly but systematically larger than those determined with the reference HNHA experiment. Conclusions about the relative precision of these experiments cannot be drawn, as the scatter results from imprecision in both experiments. It should be noted that different protein samples, $^{13}C,^{15}N$ doubly labeled and ^{15}N singly labeled, were used for acquisition of the former and latter spectrum, respectively. Both experiments underestimate the true couplings primarily because of proton spin flips occurring during the de- and rephasing periods (Δ and Δ'). Provided that selective longitudinal ^1H relaxation times are known, this effect can be accounted for.[11,12,14]

Figure 4A shows the experimental $^3J_{HN,H\alpha}$ values, corrected using experimental T_{1sel} times, plotted against high-resolution flavodoxin X-ray[30] and NMR[31] derived ϕ angles. $^3J_{HN,H\alpha}$

(24) Peng, J. W.; Wagner, G. *J. Magn. Reson.* **1992**, *98*, 308−332.
(25) Boucher, W.; Laue, E. D.; Campbell-Burk, S.; Domaille, P. J. *J. Am. Chem. Soc.* **1992**, *114*, 2262−2264.
(26) (a) Griffey, R. H.; Redfield, A. G. *Q. Rev. Biophys.* **1987**, *19*, 51−82. (b) Seip, S.; Balbach, J.; Kessler, H. *J. Magn. Reson.* **1992**, *100*, 406−410. (c) Grzesiek, S.; Bax, A. *J. Biomol. NMR* **1995**, *6*, 335−339. (d) Yamazaki, T.; Tochio, H.; Furui, J.; Aimoto, S.; Kyogoku, Y. *J. Am. Chem. Soc.* **1997**, *119*, 872−880. (e) Swapna, G. V. T.; Rios, C. B.; Shang, Z.; Montelione, G. T. *J. Biomol. NMR* **1997**, *9*, 105−111. (f) Marino, J. P.; Diener, J. L.; Moore, P. B.; Griesinger, C. *J. Am. Chem. Soc.* **1997**, *119*, 7361−7366. (g) Tessari, M.; Gentile, L. N.; Taylor, S. J.; Shalloway, D. I.; Nicholson, L. K.; Vuister, G. W. *Biochemistry* **1997**, *36*, 14561−14571. (h) Sklenář, V.; Dieckmann, T.; Butcher, S. E.; Feigon, J. *J. Magn. Reson.* **1998**, *130*, 119−124. (i) Gschwind, R. M.; Gemmecker, G.; Kessler, H. *J. Biomol. NMR* **1998**, *11*, 191−198.
(27) Palmer, A. G., III; Cavanagh, J.; Wright, P. E.; Rance, M. *J. Magn. Reson.* **1991**, *93*, 151−170.
(28) Kay, L. E.; Keifer, P.; Saarinen, T. *J. Am. Chem. Soc.* **1992**, *114*, 10663−10665.
(29) (a) Harbison, G. S. *J. Am. Chem. Soc.* **1993**, *115*, 3026−3027. (b) Norwood, T. J. *J. Magn. Reson., A* **1993**, *101*, 109−112.

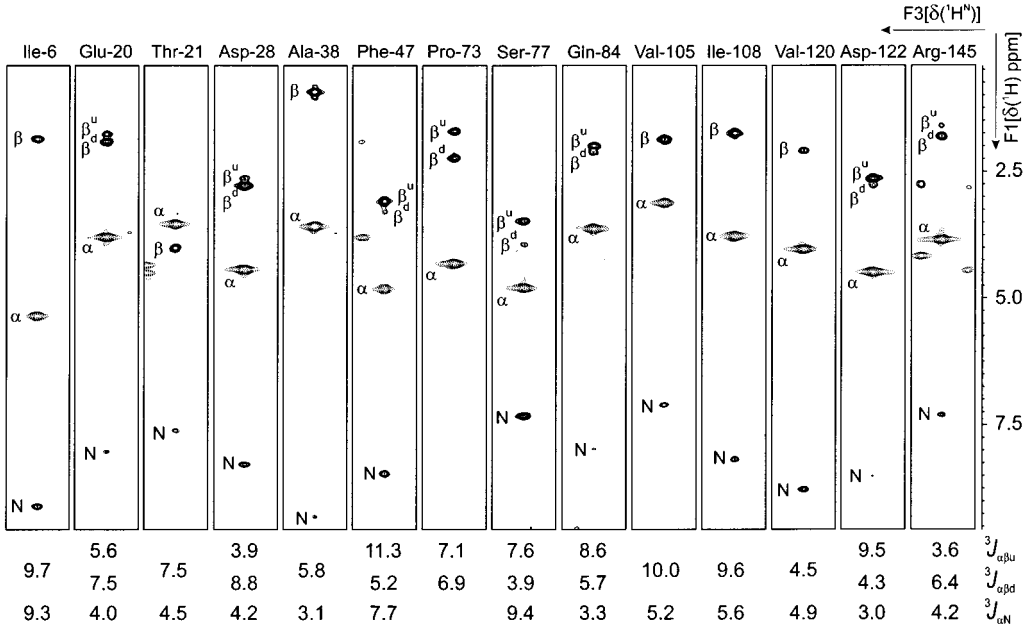

Figure 2. Strips from F1/F3 slices of a 3D HA[HB,HN](CACO)NH spectrum of $^{13}C/^{15}N$ labeled flavodoxin taken at the ^{15}N (F2) chemical shifts and centered at the $^1H^N$ (F3) chemical shifts of the amino acids sequentially following the residues indicated at the top. The width of the strips along F3 is 0.3 ppm. Positive and negative intensities are represented by solid and dashed contours, respectively, drawn on an exponential scale with a factor of $2^{1/2}$. Labels N, α, β indicate H^N, H^α, and H^β resonance assignments, respectively. Superscripts u and d denote upfield and downfield β-proton resonances, respectively. Below each panel, ^3J values are given in hertz as calculated from the H^N/H^α or H^β/H^α peak intensity ratios without correction for passive spin flips but accounting for the D_2O content of the solvent. In the case of the alanine $^3J_{H\alpha,H\beta}$ coupling constant the β (methyl) cross-peak intensity was divided by three.

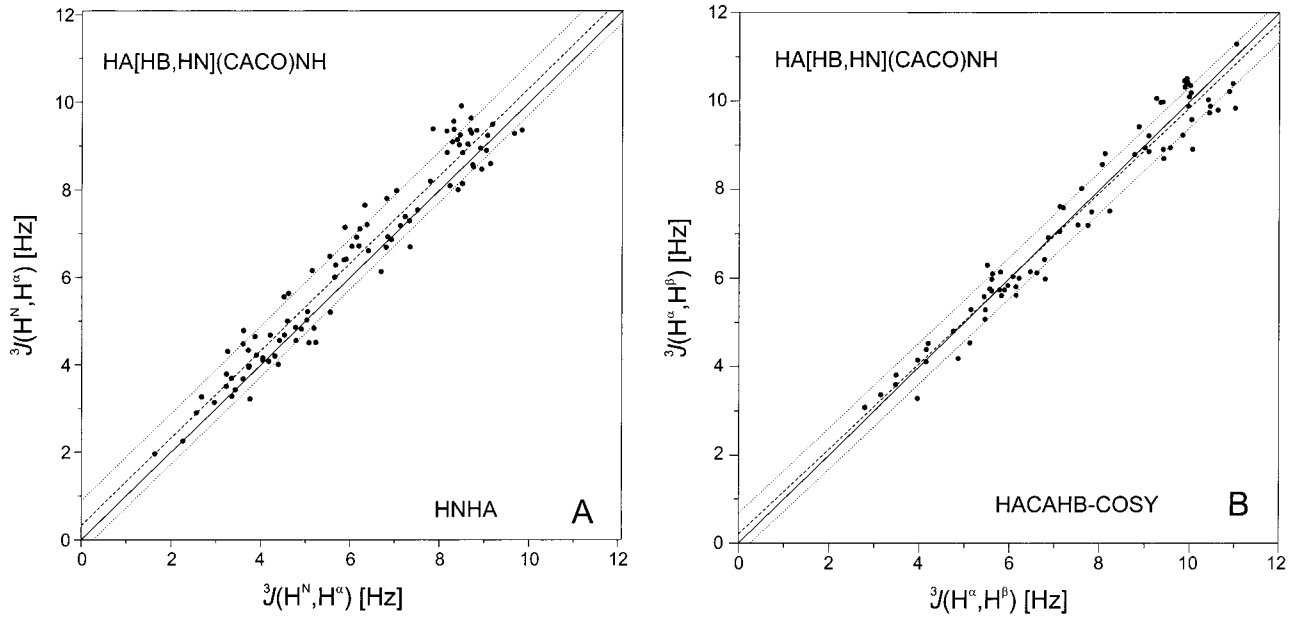

Figure 3. Comparison of $^3J_{HN,H\alpha}$ (panel A) and $^3J_{H\alpha,H\beta}$ (panel B) coupling constants in flavodoxin as determined from the HA[HB,HN](CACO)NH spectrum with reference values from HNHA and HACAHB-COSY experiments, respectively. Corrections for differential relaxation effects[29] were disregarded in all evaluations. The dashed line indicates the linear regression of coupling constants from the two respective sources with the $\pm\sigma$ boundaries represented by dotted lines. Coupling constants are calculated directly from cross/auto peak intensity ratios.

coupling constants derived from HA[HB,HN](CACO)NH agreed within 0.91 Hz (rmsd) with predictions based on the flavodoxin crystal structure[30] (1.9 Å resolution) and ubiquitin-derived Karplus parameters by Hu and Bax.[32] When referencing recent "solution" ϕ angles of flavodoxin, self-consistently determined on the exclusive basis of all six associated homonuclear and heteronuclear vicinal coupling constants,[31] the root-mean-square deviation dropped at 0.74 Hz, mainly as a result of using the same protein sample as of the present study.

$^3J_{H\alpha,H\beta}$ coupling constants from HA[HB,HN](CACO)NH agree well with values from HACAHB-COSY (Figure 3B), the empirical correlation having slope and intercept of 0.965 and 0.21 Hz, respectively, with a maximum deviation between the two data sets of 1.2 Hz. Coupling constants measured in HA-

(30) Watt, W.; Tulinsky, A.; Swenson, R. P.; Watenpaugh, K. D. *J. Mol. Biol.* **1991**, *218*, 195−208.
(31) Schmidt, J. M.; Blümel, M.; Löhr, F.; Rüterjans, H. *J. Biomol. NMR* **1999**, *14*, 1−12.
(32) Hu, S.-J.; Bax, A. *J. Am. Chem. Soc.*, **1997**, *119*, 6360−6368.

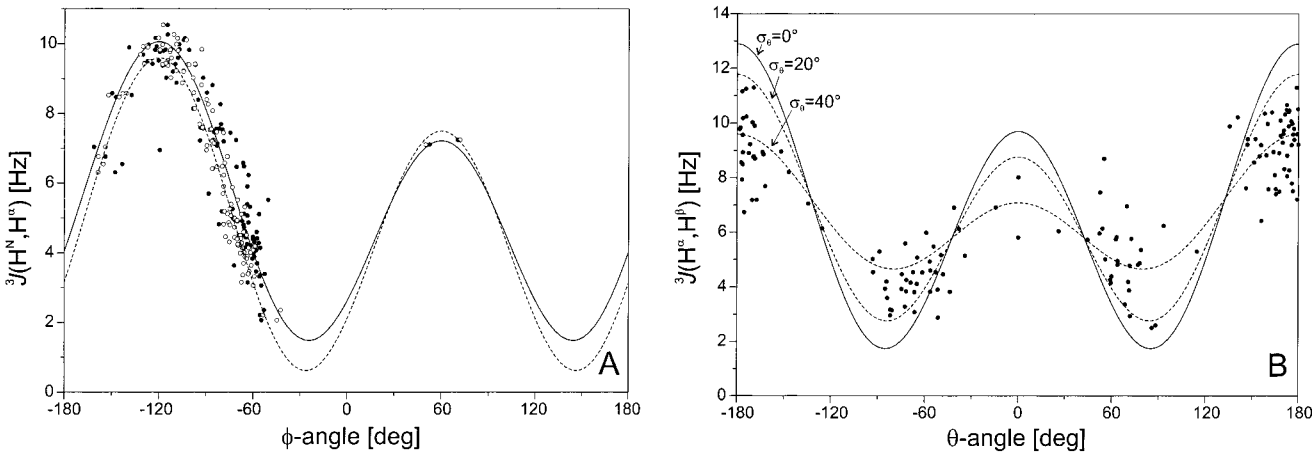

Figure 4. Correlation of coupling constants determined by the HA[HB,HN](CACO)NH method with dihedral angles in flavodoxin. In panel A $^3J_{HN,H\alpha}$ values, corrected for $^1H^N$ spin flips occurring during the *J*-evolution delays, are plotted versus ϕ angles in the crystal structure[30] (filled symbols) and "solution" ϕ angles as derived from up to six related vicinal coupling constants per residue[31] (open symbols). The solid and dashed Karplus curves[1] are represented by $^3J_{HN,H\alpha} = 7.09\cos^2(\phi - 60°) - 1.42\cos(\phi - 60°) + 1.55$ Hz[32] and $^3J_{HN,H\alpha} = 7.90\cos^2(\phi - 60°) - 1.05\cos(\phi - 60°) + 0.65$ Hz,[31] respectively. Current ^3J data from HA[HB,HN](CACO)NH seem to agree better with the Karplus curve by Hu and Bax[32] in the range of ϕ between $-100°$ and $-120°$, whereas for $\phi \approx -60°$ they seem to agree better with our recent Karplus parametrization.[31] The apparent yet negligible collective deviation was tracked down to two facts, first, that independent $^3J_{HN,H\alpha}$ coupling constants from *J*-modulated ct-HMQC[11] have been used for deriving the NMR-based (dashed) Karplus curve, and second, that backbone torsions of X-ray and NMR structures exhibit slight but genuine differences. Panel B shows the results for the side chain-conformation related $^3J_{H\alpha,H\beta}$ coupling constants. The H−C$^\alpha$−C$^\beta$−H dihedral angles θ were calculated from the crystallographic χ^1 angles of flavodoxin[30] assuming perfect tetrahedral geometry at the C$^\alpha$ and C$^\beta$ sites. Where necessary, stereospecific assignments of β-protons were derived from intraresidual NOE intensities and heteronuclear ^3J coupling information published elsewhere.[34] The solid Karplus curve is given by $^3J_{H\alpha,H\beta} = 9.5\cos^2\theta - 1.6\cos\theta + 1.8$ Hz,[35] while dashed lines show the torsion angle dependence of *J* values for various extents of χ^1 conformational mobility with Gaussian distributions of $\pm\sigma$ as indicated.

[HB,HN](CACO)NH were also compared with another data set acquired using the HC(C)H-E.COSY pulse sequence[8f] (data not shown). However, both data sets correlate with unconvincing slope and intercept of 0.69 and 2.78 Hz, respectively, reiterating that HCCH-E.COSY-type experiments very likely suffer from unwanted perturbation of passive spin states.[33] It is known[33] that, especially if couplings are small, HC(C)H-E.COSY severely understimates the true values and requires extensive amendments be made using programs not available to us. Unlike $^3J_{HN,H\alpha}$ values, $^3J_{H\alpha,H\beta}$ values from HA[HB,HN](CACO)NH were not corrected for proton spin-flip effects, because experimental $^1H^\beta$ T_{1sel} times were not available.

Rapid methyl-group rotation about the C$^\alpha$−C$^\beta$ bond in alanine residues gives rise to dynamically averaged $^3J_{H\alpha,H\beta}$ coupling constants. For the 17 alanine residues in flavodoxin, the mean $^3J_{H\alpha,H\beta}$ as determined from the HA[HB,HN](CACO)NH experiment was 5.9 ± 0.2 Hz, which agrees with data obtained for calmodulin (5.6−6.2 Hz) using the HACAHB-COSY.[15] However, commonly used Karplus parameters[35] suggest a higher value of 6.6 Hz. The experimental variation indicated above is considered the minimum random uncertainty of $^3J_{H\alpha,H\beta}$ coupling constants measured in this study because of the high signal-to-noise ratio of the C$^\beta$H$_3$ cross-peaks.

The $^3J_{H\alpha,H\beta}$ coupling constants measured in flavodoxin for residues other than alanine are plotted against the side chain conformations in the X-ray structure (Figure 4B) most of which adopt one of the three low-energy staggered rotamers. A wide distribution of *J* values is observed for gauche as well as for trans orientations of the substituents. However, conclusions on the accuracy of the *J* coupling constants obtained with the HA-[HB,HN](CACO)NH experiment must not be drawn as the critical assumption that the protein structures in solution and solid state are identical might not prevail. Such differences are generally more likely to occur in amino acid side chains than in the main chain. Accounting for differential relaxation effects cannot affect the scatter either, as the group of *J* values would only be systematically shifted to larger numbers. Stereospecific assignments, which cannot be confirmed on the basis of the X-ray structure alone, are critical as well. However, NOE measurements on flavodoxin in conjunction with the present ^3J data allow for unambiguous assignments. A considerable fraction of the experimental values encountered in the NMR study tends to intermediate values hinting at side chain conformational mobility causing dynamic averaging of *J* values.[36]

As the HA[HB,HN](CACO)NH experiment disperses auto peaks by three different resonance frequencies ($^1H^\alpha$, ^{15}N, $^1H^N$), spectral overlap in the determination of *J* values is of minor concern. This contrasts with HNHA as well as HACAHB-COSY spectra, in which reference intensities are to be taken from diagonal peaks [$^1H^N$, ^{15}N, $^1H^N$] and [$^1H^\alpha$, $^{13}C^\alpha$, $^1H^\alpha$], respectively. In addition, the resolution in the ^{15}N dimension is improved owing to the semiconstant-time[21] t_2 period, whereas in the HNHA experiment ^{15}N chemical shift and $^3J_{HN,H\alpha}$ evolve simultaneously, compromising resolution by comparatively short H^N de- and rephasing periods to limit the effect of H$^\alpha$ spin flips. Compared with HACAHB-COSY, separation of methylene $^1H^\beta$ signals is improved in HA[HB,HN](CACO)NH spectra because the t_1 acquisition time is not limited by the passive $^1J_{C\alpha,C\beta}$ interaction. It should be noted, however, that t_1 has to be much shorter than the inverse of the homonuclear couplings involving amide, α, and β protons to avoid significant differences in line

(33) (a) Zimmer, D. P.; Marino, J. P.; Griesinger, C. *Magn. Reson. Chem.* **1996**, *34*, S177−S186. (b) Carlomagno, T.; Schwalbe, H.; Rexroth, A.; Sørensen, O. W.; Griesinger, C. *J. Magn. Reson.* **1998**, *135*, 216−226.

(34) Löhr, F.; Pérez, C.; Schmidt, J. M.; Rüterjans, H. *Bull. Magn. Reson.* **1999**, *20*, 9−14.

(35) DeMarco, A.; Llinás, M.; Wüthrich, K. *Biopolymers* **1978**, *17*, 617−636.

(36) (a) Jardetzky, O. *Biochim. Biophys. Acta* **1980**, *621*, 227−232. (b) Hoch, J. C.; Dobson, C. M.; Karplus, M. *Biochemistry* **1985**, *24*, 3831−3841. (c) Brüschweiler, R.; Case, D. A. *J. Am. Chem. Soc.* **1994**, *116*, 11199−11200.

shapes which would lead to erroneous coupling constants when relying on cross-peak and auto peak heights rather than on integrated signal intensities.

Shortcomings of the HA[HB,HN](CACO)NH sequence are inherent to its magnetization transfer pathway preventing ^3J data for the C-terminal amino acid and for residues preceding prolines from being obtained. In comparison with HNHA and, if applied to a protein sample dissolved in D_2O, HACAHB-COSY experiments, both of which employ a unidirectional in-phase COSY magnetization transfer to a single spin neighbor, the simultaneous dephasing of α-proton magnetization with respect to two adjacent homonuclear spins in a linear coupling network inevitably leads to reduced diagonal and cross-peak intensities in HA[HB,HN](CACO)NH spectra. Given the chosen de- and rephasing delays and amino acid coupling constants of $^3J_{HN,H\alpha} = 9$ Hz, $^3J_{H\alpha,H\beta 2} = 11$ Hz, and $^3J_{H\alpha,H\beta 3} = 4$ Hz, the signal-to-noise ratio typically decreases at 66% and 78% for the determination of $J_{HN,H\alpha}$ and $J_{H\alpha,H\beta}$, respectively. On the other hand, the feature of simultaneous evolution of both correlations allows the measurement of different coupling types in a single rather than two experiments, thus producing a gain in measuring time and making sample handling more convenient.

Concluding Remarks

A pulse sequence has been presented for measuring two types of scalar coupling constants relevant to restraining of both ϕ- and χ^1-torsion angles in protein-structure calculations. The accuracy could be assessed by comparison with established methods and in the case of $^3J_{HN,H\alpha}$ by correlation with independently determined ϕ angles via the Karplus relation. Compared to previously published versions of quantitative homonuclear *J* correlation experiments an inherently higher resolution is achieved, although at a reduced signal-to-noise ratio due to the larger number of coherence transfer steps. For a 16-kDa protein dissolved in water at moderate concentration, the number of signals evaluated, in particular those relevant to $^3J_{H\alpha,H\beta}$ coupling constants, was larger than with any other method.

Acknowledgment. We thank Prof. S. G. Mayhew (Department of Biochemistry, University College Dublin) and Dr. M. Knauf for their support with the expression and labeling of the *D. vulgaris* flavodoxin. The help of Dr. M. Blümel in the determination of $^3J_{H\alpha,H\beta}$ coupling constants from the HC(C)H-E.COSY spectrum is gratefully acknowledged. This work was supported by a grant from the Deutsche Forschungsgemeinschaft (Ru 145/11-2).

JA991356H